ACS APPLIED NANO MATERIALS

www.acsanm.org Article

Patterned Carbon Nanotube Bundles as Stretchable Strain Sensors for Human Motion Detection

Kwanhun Kim,[‡] Jaeyong Lee,[‡] Eunhwan Jo, Sangjun Sim, and Jongbaeg Kim*

Cite This: *ACS Appl. Nano Mater.* 2020, 3, 11408−11415 Read Online

ACCESS | Metrics & More | Article Recommendations | Supporting Information

ABSTRACT: Although numerous studies have been conducted to develop wearable strain sensors with high sensitivity and a wide detection range, developing strain sensors with tunable sensitivity for practical purposes remains challenging. Strain sensors with tunable sensitivity have great potential in applications such as human motion detection and health monitoring. This paper introduces strain sensors that adopt zigzag-patterned carbon nanotube (CNT) bundle arrays embedded in a polymer matrix. Owing to the zigzag pattern, the sensors exhibited an extensive detection range up to 500% strain and high sensitivity (gauge factor of 64.08). In this study, the CNT bundle array synthesized on a Si wafer was transferred to a silicone elastomer substrate using a roll-transfer technique, forming a sheet-like structure of overlapped CNT bundles. The separation occurring between the CNT bundles with the applied strain followed the shape of the zigzag pattern. The sensors exhibited excellent repeatability and durability with negligible hysteresis behavior, and their sensitivity was tunable based on the pattern design. Furthermore, this study investigated the sensing mechanism of the sensors and their potential use in wearable electronics.

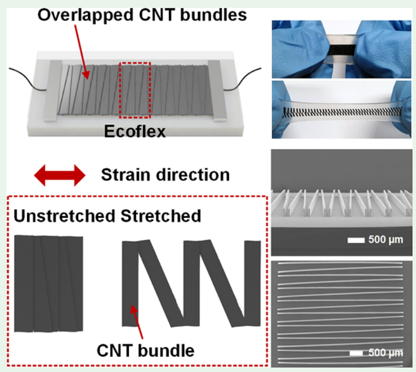

KEYWORDS: *stretchable electronics, strain sensors, carbon nanotubes, tunable sensitivity, human motion detection*

■ INTRODUCTION

Flexible and stretchable electronic devices have received considerable attention for their wide application areas such as flexible displays,[1,2] soft robotics,[3,4] health monitoring,[5,6] and human−machine interfaces.[7−9] Stretchable strain sensors are particularly important because of their use in wearable devices for health monitoring or human motion detection.[10−15] For use in these applications, strain sensors require high sensitivity and a wide detection range.[16] For instance, vital signs such as blood pressure, pulse rate, and respiratory rates cause subtle physical movements, and therefore, strain sensors with high sensitivity (gauge factor (GF) ≥20; GF is defined as the relative change in resistance per unit strain) are needed to monitor these health-related conditions.[17] In addition, strain sensors with a broad sensing range (>100%) are desired to measure extensive body motions, including bending and straightening of joints.[14] Because conventional strain gauges are composed of metal foils or semiconductors, their brittleness and rigidity limit their flexibility, which renders them unsuitable for such health-monitoring applications.[18,19]

Recently, flexible strain sensors have been developed by integrating conductive nanomaterials such as metal nanowires,[20−23] metal nanoparticles,[24,25] graphene,[26−29] and carbon nanotubes (CNTs)[30−33] with elastomers. Despite their achievements, developing sensors that simultaneously satisfy both the requirements (high sensitivity and a broad detection range) remain challenging.[16,24] For example, a crack-based sensor comprising a thin Pt film deposited on a polymer exhibited an extremely high GF (over 2000); however, it had a limited working range (0−2% strain).[24] In another study, a highly stretchable strain sensor comprising aligned CNT fibers and a prestrained flexible substrate achieved a strain range up to 900%,[30] while its GF was less than 1 for the strain range of 0−400%. Likewise, there is a trade-off between the sensitivity and detection range of the sensor, which limits its application in wearable sensors.[14,17] Therefore, it is necessary to develop strain sensors with an appropriate sensing range and sensitivity for different target applications.

Numerous studies were conducted to adjust the sensitivity or sensing range of strain sensors to meet the requirements of wearable applications.[33−39] For instance, the strain sensitivity of the sensors was effectively tuned by customizing the composition of conductive polymer composites.[33−35] A strain sensor based on a multiwalled CNT (MWCNT)/polymer fiber with tunable sensitivity (GF 25−160) by varying the content of the MWCNT was reported.[33] Sensitivity tuning of strain sensors was also achieved by employing microscopic

Received: September 15, 2020
Accepted: October 7, 2020
Published: October 20, 2020

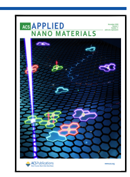

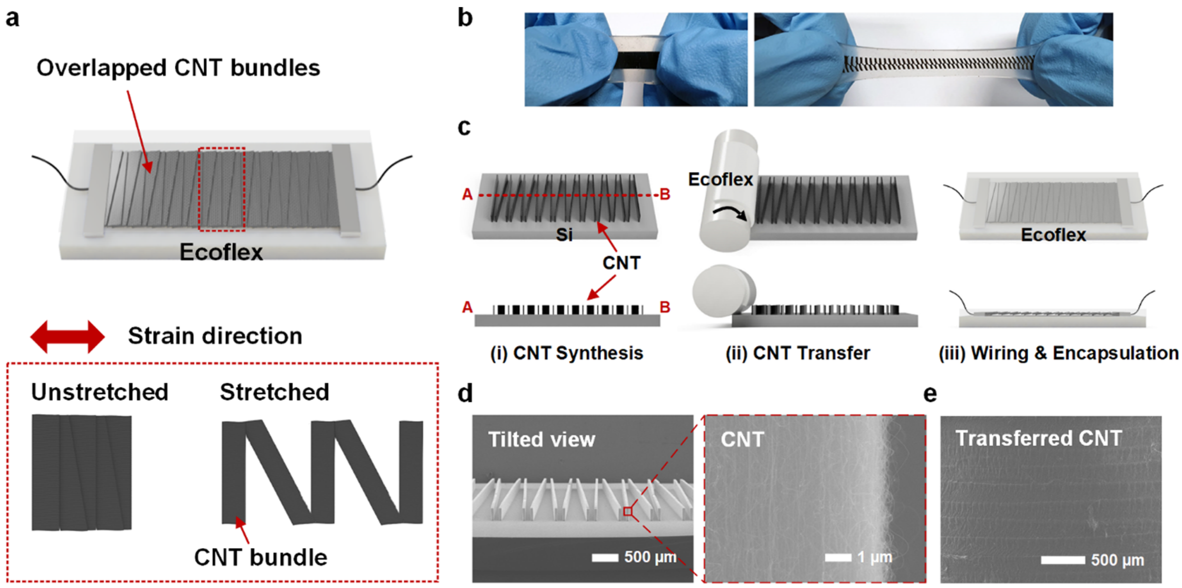

Figure 1. (a) Schematic of the fabricated strain sensor. (b) Optical images of the fabricated sensor at unstretched and stretched states. (c) Schematics of the fabrication process of the proposed sensor. (d) SEM images of the zigzag-patterned CNT bundle array synthesized on a Si wafer before the roll-transfer process. (e) SEM image of the patterned CNT bundle array after the roll-transfer process. The CNT bundles overlap with adjacent bundles, forming a sheet-like structure.

morphology and structure effects on the sensor.[37−39] For example, GFs of 3D printed graphene/polymer composite strain sensors were controlled by varying the filament thickness or its porous structure.[37,38] Although these studies achieved the tunable sensing performance of strain sensors, they involved a time-consuming adjustment of fabrication processes. Therefore, strain sensors with a simple design and scalable fabrication process are needed.

Here, we introduce a highly stretchable strain sensor with tunable sensitivity and a strain range up to 500%. The sensor consists of a zigzag-patterned CNT bundle array embedded in a polymer matrix. The CNTs were synthesized on a silicon wafer by a chemical vapor deposition (CVD) method and then transferred to an Ecoflex substrate by a roll-transfer process to form a sheet-like structure.[40,41] The sensor sensitivity was tuned by varying the pattern designs of the CNT bundle arrays, and multiple sensors with differently tuned sensitivities were obtained in a single fabrication process. Based on the pattern design, the fabricated sensor exhibited an adjustable GF ranging between 0.51 and 64.08. In addition, an extensive detection range was achieved owing to the zigzag pattern. The sensor showed negligible hysteresis behavior along with excellent repeatability and durability against a cyclic strain. We also studied the sensing mechanism of the sensor based on zigzag patterns of the CNT bundle array and the overlapped area between the adjacent CNT bundles. We successfully measured both subtle movements, such as wrist pulses, and extensive motions, such as joints bending, to demonstrate potential use of strain sensors in wearable electronics.

RESULTS AND DISCUSSION

Design and Fabrication. A schematic of the proposed strain sensor is illustrated in Figure 1a. The sensor consists of a zigzag-patterned CNT bundle array transferred to and embedded in the Ecoflex matrix. Once the array is transferred, CNT bundles overlap with one another while maintaining the zigzag pattern. With the applied tensile strain, the overlapped area is reduced, creating a gap between the CNT bundles. However, both ends of the CNT bundles retain the overlapped regions with adjacent bundles even under large deformations owing to the zigzag pattern design. Figure 1b shows optical images of the fabricated sensor under unstretched and stretched conditions.

For sensor fabrication, a patterned CNT bundle array was first synthesized on a Si wafer by the CVD process (Figure 1c). A catalyst (Fe) for the CNT synthesis was deposited on the Si wafer and patterned with the photolithography and lift-off processes. Figure 1d shows the scanning electron microscopy (SEM) image of the synthesized CNT bundle array viewed from a tilted angle. It confirms a well-defined zigzag pattern of the CNT bundle array, as designed in the catalyst patterning step. The synthesized CNT bundle array was then transferred to an Ecoflex substrate using a roll-transfer technique,[40,41] as shown in the SEM image of Figure 1e. The CNT bundles lay down and get overlapped with the adjacent bundles due to the force applied by the roller while maintaining their zigzag patterns (Figure S1, Supporting Information).[42,43] After the electrical wires were connected to the transferred CNT bundle array using a colloidal silver liquid, the CNT/Ecoflex composite was encapsulated by pouring liquid Ecoflex mixture followed by curing at room temperature. Owing to the scalability of the manufacturing methods, CVD of vertically aligned CNTs[44,45] and roll-transfer technique,[40,43] multiple sensors with different pattern designs (sensitivity determining factor) could be fabricated in a single process. (Figure S2, Supporting Information).

Strain-Sensing Characteristics. To investigate strain-sensing characteristics of the sensor, the electrical resistance of the sensor with θ = 2.30° was measured while varying the applied strain. Here, θ refers to the angle of the inclined lines in the zigzag pattern (Figure S3, Supporting Information). The experimental setup is illustrated in Figure S4 (Supporting Information). Figure 2a depicts the relative resistance change of the sensor ($\Delta R/R_0$) for various strain values, where ΔR represents the change in the resistance of the sensor induced

https://dx.doi.org/10.1021/acsanm.0c02494
ACS Appl. Nano Mater. 2020, 3, 11408−11415

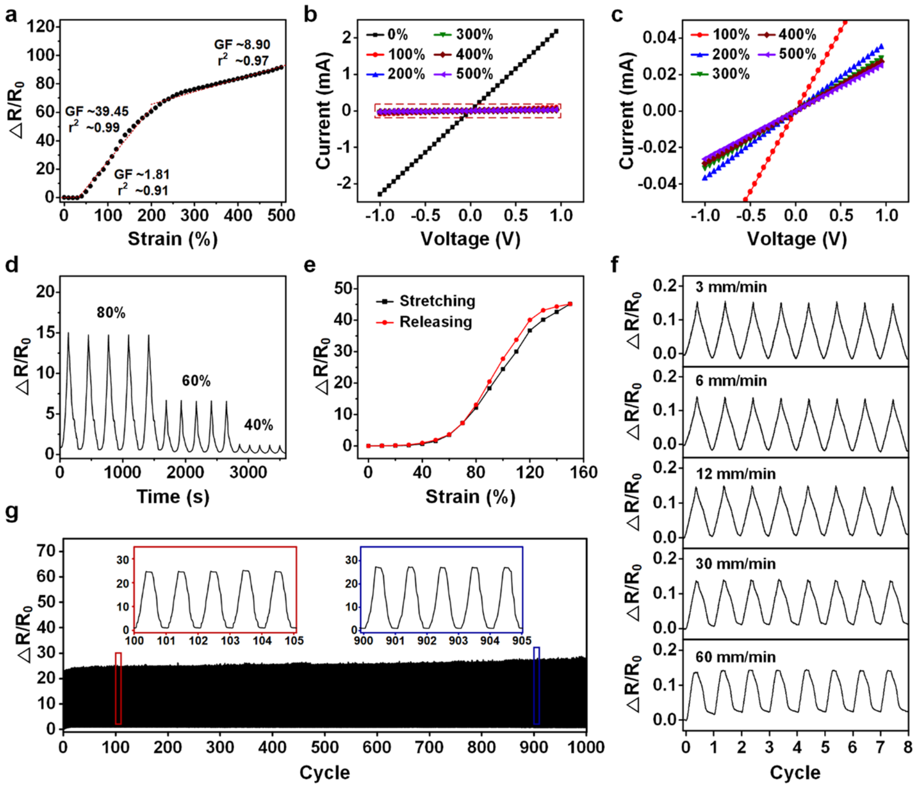

Figure 2. Strain-sensing characteristics of the proposed sensor. (a) Relative resistance changes of the sensor for varying strain values. (b) I−V curves of the sensor for various strain values. (c) Magnified plot of the I−V curves. (d) Dynamic sensor response to repeated strain values of 80, 60, and 40%. (e) Relative resistance changes of the sensor during stretch (black) and release (red) for up to 150% strain. (f) Response of the sensor to repeated strain values of 20% at various strain rates. (g) Sensor response to 100% cyclic strain repeated for 1000 cycles. The insets show the sensor response for five consecutive cycles in the 100th and 900th cycle.

by the application of strain and R_0 is the sensor resistance before elongation. It can be seen that the value of the relative resistance change increases with the applied strain, and the sensing curve indicates three linear regions: 0−40% ($r^2 \approx 0.91$), 40−200% ($r^2 \approx 0.99$), and 200−500% ($r^2 \approx 0.97$). The sensor exhibited GFs of 1.81, 39.45, and 8.90 for the strain regions of 0−40, 40−200, and 200−500%, respectively. Figure S5 indicates that the sensor is extremely stretchable with strain up to 500%. Figure 2b,c shows that the I−V curves exhibit a linear response for strain values ranging between 0 and 500%, confirming the stable electrical contact of the sensor. We also examined the sensor response to repeated cycles of 80, 60, and 40% strain (Figure 2d). The output responses were highly consistent, justifying the reliability and repeatability of the sensor. Figure 2e shows that the sensor exhibits negligible hysteresis behavior at the relative resistance change corresponding to the strain range of 0−150%. Hysteresis behavior at large strain levels can be attributed to the viscoelasticity of Ecoflex and the low interfacial adhesion between the CNTs and elastomer matrix,[46,47] which can be resolved by introducing proper adhesive materials.[48] We further investigated the influence of strain rates (3, 6, 12, 30, and 60 mm/min) on the sensing properties at a cyclic strain of 20% (Figure 2f). The resistance changes were uniform, indicating the stability of the sensor with respect to the strain rate. Finally, to evaluate the sensor's reliability for practical applications, the dynamic durability and response time of the sensor were examined. A cyclic strain of 100% was applied for over 1000 cycles to assess the durability of the sensor (Figure 2g). The sensor maintained a stable response without a measurable indication of degradation. A 10% strain applied to the sensor at a high strain rate (100 mm/s) (Figure S6, Supporting Information) led to the response time of approximately 56 ms, which was comparable to that of state-of-the-art strain sensors.[49−52]

Sensing Mechanism. We performed a finite element method (FEM) analysis to verify the sensing mechanism of strain sensors. Note that the current path changes characteristically with increased strain, as shown in Figure S7 (Supporting Information). Figure 3a illustrates how the current path changes as the strain is induced. Typically, the resistance (R) of a given object is expressed as $R = \rho(l/A)$, where ρ is the electrical resistivity, l is the length, and A is the cross-sectional area of the conductor (or a resistor). In the small strain range where only sliding between adjacent CNT bundles occurred, the resistance changed slightly owing to the elongation of the active length (l) of the conduction path. With the continuously applied strain, the CNT bundles began to partially separate, reducing the active cross-sectional area of the current path and consequently increasing the sensor resistance. The zigzag pattern caused the gradual separation of CNT bundles. When adjacent CNT bundles were separated beyond the midpoint, the total length (l) of the current path increased significantly along the zigzag pattern until only the ends of the CNT bundle were left overlapping. Also, the width of the cross-sectional area A is reduced to the length of the CNT bundle width, which is defined by the length of the synthesized CNTs. This drastically increased the resistance for the maximum GF of the sensor (strain region of 40−200% in Figure 2a). However, the overlapped portions of both ends of the CNT bundles

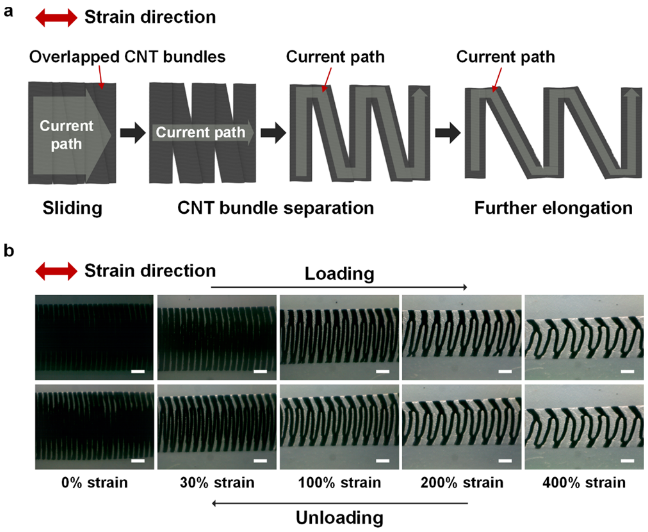

Figure 3. Strain-sensing mechanism of the sensor. (a) Schematics illustrating the change in morphology of the overlapped CNT bundles as strain increases. The CNT bundles separate, forming the zigzag pattern. (b) Optical images of the sensor at various strain values, when stretched up to 400% strain and then released (scale bar: 1 mm).

remained overlapped even for a very large (~500% strain) applied strain. This can be attributed to the spatially nonuniform elastic properties of heterogeneous composites that result in varying local strain at specific locations depending on the elastic modulus.[17,53] Because Young's modulus values of CNTs (270−950 GPa)[54] are several orders of magnitude higher than that of Ecoflex (~0.1 MPa),[55,56] the area containing the CNT bundles has a higher local modulus of elasticity than the area consisting of Ecoflex only. Thus, a relatively small amount of local strain was induced where the overlapped CNT bundles were located.

Figure 3b shows optical images of the morphology of the transferred CNT array for different strain values to validate the sensing mechanism. In the initial state where no strain was applied, CNT bundles overlapped with one another forming a sheet-like structure. As the sensor was stretched to 30% strain, partial separation occurred between the adjacent bundles. Under larger strain values, the CNT bundles were disconnected, except at the edges, where they maintained their positions and the overlap forming a zigzag pattern. In contrast to our previous work, wherein we used a parallel line pattern resulting in a relatively narrow sensing range induced by the electrical disconnection of CNT bundles,[40] the applied zigzag pattern allowed for the measurement of a wide strain range. Upon release, the separated CNT bundles retained their initial positions, restoring the electrical resistance.

The sensing mechanism of the proposed sensor is different from that of a randomly distributed CNT−polymer composite-based strain sensor. In the case of randomly distributed CNT-polymer composites, the resistance change was mainly due to the decrease in the number of CNT−CNT contacts, and this change was more severe near the percolation threshold.[57] The disconnection between CNTs sharply increased the resistance leading to a strain range with the highest GF, but only over a short strain interval just before the sensor reached an insulating state.[33] This sudden increase in resistance just before the electrical disconnection of the sensor makes it difficult to operate the sensor in the most sensitive strain ranges suitable for various applications. However, by utilizing our proposed strain sensor, the sensor can be designed to have the highest GF in the strain range for use in the desired applications.

Sensitivity Tuning. To investigate the effect of the pattern shape on the sensor sensitivity, we designed zigzag patterns with different angles (θ: 1.15, 2.30, 2.86, and 3.45°) between the nearby CNT bundles (Figure 4a,b). The CNT length was approximately 300 μm for all the four pattern designs. Details of the designs are illustrated in Figure S3 (Supporting Information). Depending on θ, the overlapped area between

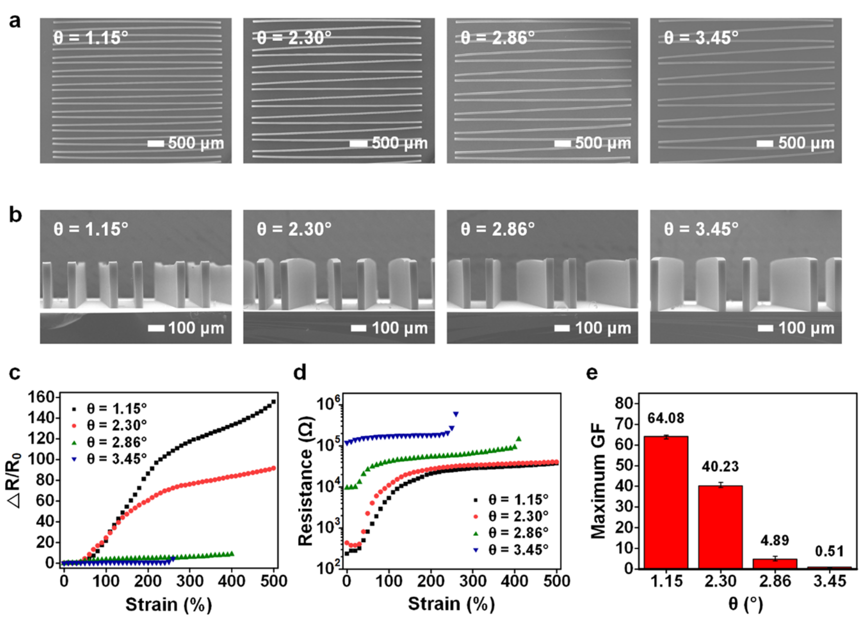

Figure 4. (a) Top- and (b) side-view SEM images of the CNT bundle array with varying θ values, before the roll-transfer process. (c) Relative resistance changes of the sensors with different θ values under the applied strain. (d) Strain-sensing responses of the sensors fabricated with different pattern designs. (e) Maximum GF exhibited by the sensors designed with different θ values of 1.15, 2.30, 2.86, and 3.45°.

https://dx.doi.org/10.1021/acsanm.0c02494
ACS Appl. Nano Mater. 2020, 3, 11408−11415

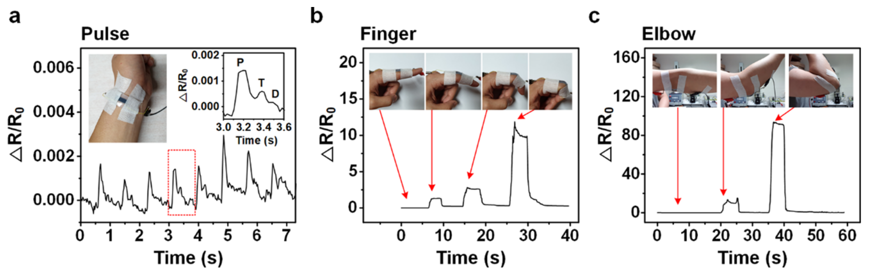

Figure 5. Applications of the sensor for human motion detection. (a) Sensor response to wrist pulses. (b, c) Relative resistance changes of the sensor to (b) finger and (c) elbow motion at various degrees of bending.

CNT bundles varied, allowing for the fabrication of sensors with different degrees of separation between the bundles at a given strain. Because the strain-induced resistance change of the sensor is primarily due to the separation of the CNT bundles and the change in current path geometry (Figure 3a),[40,58,59] the strain-sensing performance could be adjusted with a simple modification of θ.

Figure 4c,d depicts the sensor response under various strain conditions for each pattern design. The sensor with $\theta = 1.15°$ exhibited the highest GF (64.08), followed by $\theta = 2.30°$ (GF ~ 40.23). However, sensors with θ values of 2.86 and 3.45° showed relatively low GFs: 4.89 and 0.51, respectively (Figure 4e). This can be attributed to the high initial resistance of the sensors due to the less overlapped area (Figure S8, Supporting Information), and the smaller amount of separation occurred between the CNT bundles at a given strain value.

With respect to the sensing range, sensors with θ values of 1.15 and 2.30° could detect up to 500% strain, while sensors with θ values of 2.86 and 3.45° exhibit a relatively narrow detection range. This is because sensors with a large θ have a small overlapped area of CNT bundles; thus, a large deformation separates adjacent CNT bundles even at their ends, causing an electrical disconnection of the sensor (Figure S9, Supporting Information). Nevertheless, we can design our sensors to have GFs in the range of 0.51 to 64.08 with a maximum detection range of 500% strain. This is a highly sensitive sensor with an extensive sensing range compared with state-of-the-art conductive nanomaterial−polymer composite-based strain sensors (Figure S10 and Table S1, Supporting Information).

Applications. The fabricated sensor was demonstrated to be a wearable device for human motion detection (Figure 5). High sensitivity and stretchability of the sensor enabled the measurement of a wide range of human motions, from subtle movements, such as wrist pulses, to extensive movements, such as joint bending motion. The sensors were attached to the subject's skin using a commercial medical tape, and the electrical output signals were monitored during these physical movements. As shown in Figure 5a, the wrist pulse signals can be clearly measured, with the ability to distinguish the characteristic waveforms such as percussion, tidal, and diastolic waves. Considering that one's physical condition can be extracted from monitoring physiological responses,[13] the sensor could also be used in the diagnostic or rehabilitation applications. For extensive motion detection, the sensor was attached to the subject's finger and elbow, and the signal was measured according to the joint movements. Figure 5b,c shows that the sensor can distinguish the degree of bending by monitoring the corresponding change in relative resistance. The proposed sensor can successfully detect both subtle and extensive human motions, indicating its potential use in various applications.

CONCLUSIONS

We introduced highly stretchable and sensitive strain sensors based on zigzag-patterned CNT bundle arrays. A roll-transfer process was used to transfer the CNT bundles to the silicone elastomer while maintaining the array pattern design. We found that the sensor sensitivity can be tuned by varying the zigzag pattern design, which enabled the sensors to have GF values from 0.51 to 64.08. We used a scalable fabrication process to demonstrate that strain sensors with differently tuned sensitivities can be obtained in a single manufacturing process. The sensors exhibited excellent strain sensing performance including an extensive detection range up to 500% strain, outstanding repeatability, negligible hysteresis, and durability. When used as a wearable sensor for human motion detection, the sensors successfully measured both subtle and extensive physical motions, demonstrating their potential for use in diagnostic, rehabilitation, and health-monitoring applications.

EXPERIMENTAL SECTION

Synthesis of Zigzag-Patterned CNT Bundle Arrays. A zigzag-patterned CNT bundle array was synthesized on a Si wafer by CVD. First, a 3 nm-thick e-beam evaporated Fe catalyst layer was selectively deposited on a Si wafer by the lift-off process using a negative photoresist (DNR-L300; Dongjin Semichem Inc.). After heating the sample to 720 °C under the flow of 100 sccm nitrogen (N_2), it was treated with 100 sccm ammonia (NH_3) for 30 min. The CNT growth process was carried out for 15 min using 30 sccm acetylene (C_2H_2) as a precursor. Then, the sample was cooled down to room temperature in N_2.

Sensor Fabrication. The Ecoflex (00−30, Smooth-on) substrate was obtained by mixing the prepolymer and cross-linker at 1:1 wt %, followed by degassing in vacuum for 10 min. Next, 10 mL of this liquid Ecoflex was poured into a 125 mm × 125 mm square Petri dish and cured overnight. The as-synthesized patterned CNT bundle array was then transferred to the cured Ecoflex film by a roll-transfer technique as described in our previous work.[40] Electrical wires were connected to the transferred CNT array using a colloidal silver liquid (Pelco; Ted Pella, Inc.). Then, liquid Ecoflex (mixture of the prepolymer and cross-linker at 1:1 wt%) was poured onto the CNT/Ecoflex composite and cured at room temperature for encapsulation.

Characterization. A field emission scanning electron microscope (JEOL; IT-500HR) was used to characterize the surface morphologies of the CNT bundle arrays. Strain was applied to the sensor using a motorized linear stage (Cheung Won Mechatronics Co., South Korea) for the strain rates above 1 mm/s and a dip coater (Jaesung Engineering Co., South Korea) for the strain rates below 1 mm/s. The electrical response was measured using a sourcemeter (Keithley 2614B) under an applied voltage of 1 V.

https://dx.doi.org/10.1021/acsanm.0c02494
ACS Appl. Nano Mater. 2020, 3, 11408−11415

Finite Element Method Analysis. Three-dimensional modeling and FEM analysis were carried out using a commercial 3D CAD program (Creo Parametric 5.0) and FEM software (ANSYS Workbench 18.2), respectively. Because the purpose of the simulation was to simply verify the current flow pattern according to the morphology of the sensing area, we assumed each CNT bundle as a simple bulk conductor. Structural steel was selected for the material from the ANSYS Workbench library. A potential difference of 1 V was applied across both ends of the model to measure the current density.

■ ASSOCIATED CONTENT

Supporting Information

The Supporting Information is available free of charge at https://pubs.acs.org/doi/10.1021/acsanm.0c02494.

Comparison of strain-sensing properties of the recently reported strain sensors; images of CNTs during fabrication; photographs of miniaturized sensors for mass production; design of the zigzag pattern; experimental setup; photographs of the sensor under a strain of 0, 100, 300, and 500%; response of the sensor to 10% strain when stretched at a rate of 100 mm/s; FEM analysis explaining the strain-sensing mechanism of the sensor; optical images of sensors with different pattern designs; optical image of the sensor ($\theta = 3.45°$) at 200% strain; and comparison of maximum gauge factor and detection range of the recently reported strain sensors based on conductive nanomaterial−elastomeric composites (PDF)

■ AUTHOR INFORMATION

Corresponding Author

Jongbaeg Kim − *School of Mechanical Engineering, Yonsei University, Seoul 03722, Republic of Korea;* orcid.org/0000-0003-4434-5871; Email: kimjb@yonsei.ac.kr

Authors

Kwanhun Kim − *School of Mechanical Engineering, Yonsei University, Seoul 03722, Republic of Korea*

Jaeyong Lee − *School of Mechanical Engineering, Yonsei University, Seoul 03722, Republic of Korea*

Eunhwan Jo − *School of Mechanical Engineering, Yonsei University, Seoul 03722, Republic of Korea*

Sangjun Sim − *School of Mechanical Engineering, Yonsei University, Seoul 03722, Republic of Korea*

Complete contact information is available at: https://pubs.acs.org/10.1021/acsanm.0c02494

Author Contributions

‡K.K. and J.L. contributed equally to this work.

Notes

The authors declare no competing financial interest.

■ ACKNOWLEDGMENTS

This work was supported by the National Research Foundation of Korea (NRF) grant funded by the Korean government (MSIT) (2018R1A4A1025986).

■ REFERENCES

(1) Kim, S.; Kwon, H. J.; Lee, S.; Shim, H.; Chun, Y.; Choi, W.; Kwack, J.; Han, D.; Song, M.; Kim, S.; Mohammadi, S.; Kee, I.; Lee, S. Y. Low-Power Flexible Organic Light-Emitting Diode Display Device. *Adv. Mater.* **2011**, *23*, 3511−3516.

(2) White, M. S.; Kaltenbrunner, M.; Głowacki, E. D.; Gutnichenko, K.; Kettlgruber, G.; Graz, I.; Aazou, S.; Ulbricht, C.; Egbe, D. A. M.; Miron, M. C.; Major, Z.; Scharber, M. C.; Sekitani, T.; Someya, T.; Bauer, S.; Sariciftci, N. S. Ultrathin, Highly Flexible and Stretchable PLEDs. *Nat. Photonics* **2013**, *7*, 811−816.

(3) Bartlett, N. W.; Tolley, M. T.; Overvelde, J. T. B.; Weaver, J. C.; Mosadegh, B.; Bertoldi, K.; Whitesides, G. M.; Wood, R. A 3D-Printed, Functionally Graded Soft Robot Powered by Combustion. *Science* **2015**, *349*, 161−165.

(4) Rus, D.; Tolley, M. T. Design, Fabrication and Control of Soft Robots. *Nature* **2015**, *521*, 467−475.

(5) Yamada, T.; Hayamizu, Y.; Yamamoto, Y.; Yomogida, Y.; Izadi-Najafabadi, A.; Futaba, D. N.; Hata, K. A Stretchable Carbon Nanotube Strain Sensor for Human-Motion Detection. *Nat. Nanotechnol.* **2011**, *6*, 296.

(6) Huynh, T. P.; Haick, H. Autonomous Flexible Sensors for Health Monitoring. *Adv. Mater.* **2018**, *30*, 1802337.

(7) Lim, S.; Son, D.; Kim, J.; Lee, Y. B.; Song, J.-K.; Choi, S.; Lee, D. J.; Kim, J. H.; Lee, M.; Hyeon, T.; Kim, D.-H. Transparent and Stretchable Interactive Human Machine Interface Based on Patterned Graphene Heterostructures. *Adv. Funct. Mater.* **2015**, *25*, 375−383.

(8) Wang, J.; Lin, M.-F.; Park, S.; Lee, P. S. Deformable Conductors for Human−Machine Interface. *Mater. Today* **2018**, *21*, 508−526.

(9) Pyo, S.; Lee, J.; Kim, W.; Jo, E.; Kim, J. Multi-Layered, Hierarchical Fabric-Based Tactile Sensors with High Sensitivity and Linearity in Ultrawide Pressure Range. *Adv. Funct. Mater.* **2019**, *29*, 1902484.

(10) Wu, X.; Han, Y.; Zhang, X.; Lu, C. Highly Sensitive, Stretchable, and Wash-Durable Strain Sensor Based on Ultrathin Conductive Layer@Polyurethane Yarn for Tiny Motion Monitoring. *ACS Appl. Mater. Interfaces* **2016**, *8*, 9936−9945.

(11) Shi, X.; Liu, S.; Sun, Y.; Liang, J.; Chen, Y. Lowering Internal Friction of 0D-1D-2D Ternary Nanocomposite-Based Strain Sensor by Fullerene to Boost the Sensing Performance. *Adv. Funct. Mater.* **2018**, *28*, 1800850.

(12) Ma, J.; Wang, P.; Chen, H.; Bao, S.; Chen, W.; Lu, H. Highly Sensitive and Large-Range Strain Sensor with a Self-Compensated Two-Order Structure for Human Motion Detection. *ACS Appl. Mater. Interfaces* **2019**, *11*, 8527−8536.

(13) Patel, S.; Park, H.; Bonato, P.; Chan, L.; Rodgers, M. A Review of Wearable Sensors and Systems with Application in Rehabilitation. *J. Neuroeng. Rehabil.* **2012**, *9*, 21.

(14) Amjadi, M.; Kyung, K.-U.; Park, I.; Sitti, M. Stretchable, Skin-Mountable, and Wearable Strain Sensors and Their Potential Applications: A Review. *Adv. Funct. Mater.* **2016**, *26*, 1678−1698.

(15) Wang, C.; Xia, K.; Wang, H.; Liang, X.; Yin, Z.; Zhang, Y. Advanced Carbon for Flexible and Wearable Electronics. *Adv. Mater.* **2019**, *31*, 1801072.

(16) Zhang, M.; Wang, C.; Wang, H.; Jian, M.; Hao, X.; Zhang, Y. Carbonized Cotton Fabric for High-Performance Wearable Strain Sensors. *Adv. Funct. Mater.* **2017**, *27*, 1604795.

(17) Pan, S.; Liu, Z.; Wang, M.; Jiang, Y.; Luo, Y.; Wan, C.; Qi, D.; Wang, C.; Ge, X.; Chen, X. Mechanocombinatorially Screening Sensitivity of Stretchable Strain Sensors. *Adv. Mater.* **2019**, *31*, 1903130.

(18) Barlian, A. A.; Park, W. T.; Mallon, J. R., Jr.; Rastegar, A. J.; Pruitt, B. L. Review: Semiconductor Piezoresistance for Microsystems. *Proc. IEEE* **2009**, *97*, 513−552.

(19) Wang, C.; Li, X.; Gao, E.; Jian, M.; Xia, K.; Wang, Q.; Xu, Z.; Ren, T.; Zhang, Y. Carbonized Silk Fabric for Ultrastretchable, Highly Sensitive, and Wearable Strain Sensors. *Adv. Mater.* **2016**, *28*, 6640−6648.

(20) Amjadi, M.; Pichitpajongkit, A.; Lee, S.; Ryu, S.; Park, I. Highly Stretchable and Sensitive Strain Sensor Based on Silver Nanowire−Elastomer Nanocomposite. *ACS Nano* **2014**, *8*, 5154−5163.

(21) Lee, S.; Shin, S.; Lee, S.; Seo, J.; Lee, J.; Son, S.; Cho, H. J.; Algadi, H.; Al-Sayari, S.; Kim, D. E.; Lee, T. Ag Nanowire Reinforced Highly Stretchable Conductive Fibers for Wearable Electronics. *Adv. Funct. Mater.* **2015**, *25*, 3114−3121.

(22) Kim, K. H.; Jang, N. S.; Ha, S. H.; Cho, J. H.; Kim, J. M. Highly Sensitive and Stretchable Resistive Strain Sensors Based on Microstructured Metal Nanowire/Elastomer Composite Films. *Small* **2018**, *14*, 1704232.
(23) Zhu, G. J.; Ren, P. G.; Guo, H.; Jin, Y. L.; Yan, D. X.; Li, Z. M. Highly Sensitive and Stretchable Polyurethane Fiber Strain Sensors with Embedded Silver Nanowires. *ACS Appl. Mater. Interfaces* **2019**, *11*, 23649−23658.
(24) Kang, D.; Pikhitsa, P. V.; Choi, Y. W.; Lee, C.; Shin, S. S.; Piao, L.; Park, B.; Suh, K.-Y.; Kim, T.; Choi, M. Ultrasensitive Mechanical Crack-Based Sensor Inspired by the Spider Sensory System. *Nature* **2014**, *516*, 222.
(25) Lee, J.; Shin, S.; Lee, S.; Song, J.; Kang, S.; Han, H.; Kim, S.; Kim, S.; Seo, J.; Kim, D.; Lee, T. Highly Sensitive Multifilament Fiber Strain Sensors with Ultrabroad Sensing Range for Textile Electronics. *ACS Nano* **2018**, *12*, 4259−4268.
(26) Li, J.; Zhao, S.; Zeng, X.; Huang, W.; Gong, Z.; Zhang, G.; Sun, R.; Wong, C.-P. Highly Stretchable and Sensitive Strain Sensor Based on Facilely Prepared Three-Dimensional Graphene Foam Composite. *ACS Appl. Mater. Interfaces* **2016**, *8*, 18954−18961.
(27) Boland, C. S.; Khan, U.; Ryan, G.; Barwich, S.; Charifou, R.; Harvey, A.; Backes, C.; Li, Z.; Ferreira, M. S.; Mobius, M. E.; Young, R. J.; Coleman, J. N. Sensitive Electromechanical Sensors Using Viscoelastic Graphene-Polymer Nanocomposites. *Science* **2016**, *354*, 1257−1260.
(28) Shi, J.; Li, X.; Cheng, H.; Liu, Z.; Zhao, L.; Yang, T.; Dai, Z.; Cheng, Z.; Shi, E.; Yang, L.; Zhang, Z.; Cao, A.; Zhu, H.; Fang, Y. Graphene Reinforced Carbon Nanotube Networks for Wearable Strain Sensors. *Adv. Funct. Mater.* **2016**, *26*, 2078−2084.
(29) Huang, T.; He, P.; Wang, R.; Yang, S.; Sun, J.; Xie, X.; Ding, G. Porous Fibers Composed of Polymer Nanoball Decorated Graphene for Wearable and Highly Sensitive Strain Sensors. *Adv. Funct. Mater.* **2019**, *29*, 1903732.
(30) Ryu, S.; Lee, P.; Chou, J. B.; Xu, R.; Zhao, R.; Hart, A. J.; Kim, S.-G. Extremely Elastic Wearable Carbon Nanotube Fiber Strain Sensor for Monitoring of Human Motion. *ACS Nano* **2015**, *9*, 5929−5936.
(31) Roh, E.; Hwang, B.-U.; Kim, D.; Kim, B.-Y.; Lee, N.-E. Stretchable, Transparent, Ultrasensitive, and Patchable Strain Sensor for Human−Machine Interfaces Comprising a Nanohybrid of Carbon Nanotubes and Conductive Elastomers. *ACS Nano* **2015**, *9*, 6252−6261.
(32) Sun, H.; Dai, K.; Zhai, W.; Zhou, Y.; Li, J.; Zheng, G.; Li, B.; Liu, C.; Shen, C. A Highly Sensitive and Stretchable Yarn Strain Sensor for Human Motion Tracking Utilizing a Wrinkle-Assisted Crack Structure. *ACS Appl. Mater. Interfaces* **2019**, *11*, 36052−36062.
(33) He, Z.; Byun, J.-H.; Zhou, G.; Park, B.-J.; Kim, T.-H.; Lee, S.-B.; Yi, J.-W.; Um, M.-K.; Chou, T.-W. Effect of MWCNT Content on the Mechanical and Strain-Sensing Performance of Thermoplastic Polyurethane Composite Fibers. *Carbon* **2019**, *146*, 701−708.
(34) Liu, H.; Li, Q.; Bu, Y.; Zhang, N.; Wang, C.; Pan, C.; Mi, L.; Guo, Z.; Liu, C.; Shen, C. Stretchable Conductive Nonwoven Fabrics with Self-Cleaning Capability for Tunable Wearable Strain Sensor. *Nano Energy* **2019**, *66*, 104143.
(35) Yang, K.; Yin, F.; Xia, D.; Peng, H.; Yang, J.; Yuan, W. A Highly Flexible and Multifunctional Strain Sensor Based on a Network-Structured MXene/Polyurethane Mat with Ultra-High Sensitivity and a Broad Sensing Range. *Nanoscale* **2019**, *11*, 9949−9957.
(36) Tao, L. Q.; Wang, D. Y.; Tian, H.; Ju, Z. Y.; Liu, Y.; Pang, Y.; Chen, Y. Q.; Yang, Y.; Ren, T. L. Self-Adapted and Tunable Graphene Strain Sensors for Detecting Both Subtle and Large Human Motions. *Nanoscale* **2017**, *9*, 8266−8273.
(37) Huang, K.; Dong, S.; Yang, J.; Yan, J.; Xue, Y.; You, X.; Hu, J.; Gao, L.; Zhang, X.; Ding, Y. Three-Dimensional Printing of a Tunable Graphene-Based Elastomer for Strain Sensors with Ultrahigh Sensitivity. *Carbon* **2019**, *143*, 63−72.
(38) Wang, Z.; Zhang, Q.; Yue, Y.; Xu, J.; Xu, W.; Sun, X.; Chen, Y.; Jiang, J.; Liu, Y. 3D Printed Graphene/Polydimethylsiloxane Composite for Stretchable Strain Sensor with Tunable Sensitivity. *Nanotechnology* **2019**, *30*, 345501.
(39) Yang, S.; Li, C.; Cong, T.; Zhao, Y.; Xu, S.; Wang, P.; Pan, L. Sensitivity-Tunable Strain Sensors Based on Carbon Nanotube@ Carbon Nanocoil Hybrid Networks. *ACS Appl. Mater. Interfaces* **2019**, *11*, 38160−38168.
(40) Lee, J.; Pyo, S.; Kwon, D.-S.; Jo, E.; Kim, W.; Kim, J. Ultrasensitive Strain Sensor Based on Separation of Overlapped Carbon Nanotubes. *Small* **2019**, *15*, 1805120.
(41) Lee, J.; Pyo, S.; Jo, E.; Kim, J. Development of a Highly Stretchable Strain Sensor Based on Patterned and Rolled Carbon Nanotubes. *2019 IEEE 32nd International Conference on Micro Electro Mechanical Systems (MEMS)*. IEEE: Seoul, Korea (South), 2019, pp. 811−814.
(42) Pint, C. L.; Xu, Y.-Q.; Pasquali, M.; Hauge, R. H. Formation of Highly Dense Aligned Ribbons and Transparent Films of Single-Walled Carbon Nanotubes Directly from Carpets. *ACS Nano* **2008**, *2*, 1871−1878.
(43) Tawfick, S.; O'Brien, K.; Hart, A. J. Flexible High-Conductivity Carbon-Nanotube Interconnects Made by Rolling and Printing. *Small* **2009**, *5*, 2467−2473.
(44) Zhang, Q.; Huang, J.-Q.; Zhao, M.-Q.; Qian, W.-Z.; Wei, F. Carbon Nanotube Mass Production: Principles and Processes. *ChemSusChem* **2011**, *4*, 864−889.
(45) Wang, M.; Li, T.; Yao, Y.; Lu, H.; Li, Q.; Chen, M.; Li, Q. Wafer-Scale Transfer of Vertically Aligned Carbon Nanotube Arrays. *J. Am. Chem. Soc.* **2014**, *136*, 18156−18162.
(46) Ci, L.; Suhr, J.; Pushparaj, V.; Zhang, X.; Ajayan, P. M. Continuous Carbon Nanotube Reinforced Composites. *Nano Lett.* **2008**, *8*, 2762−2766.
(47) Jin, L.; Chortos, A.; Lian, F.; Pop, E.; Linder, C.; Bao, Z.; Cai, W. Microstructural Origin of Resistance−strain Hysteresis in Carbon Nanotube Thin Film Conductors. *Proc. Natl. Acad. Sci.* **2018**, *115*, 1986−1991.
(48) Lee, C.-J.; Park, K. H.; Han, C. J.; Oh, M. S.; You, B.; Kim, Y.-S.; Kim, J.-W. Crack-Induced Ag Nanowire Networks for Transparent, Stretchable, and Highly Sensitive Strain Sensors. *Sci. Rep.* **2017**, *7*, 7959.
(49) Yu, Y.; Zhai, Y.; Yun, Z.; Zhai, W.; Wang, X.; Zheng, G.; Yan, C.; Dai, K.; Liu, C.; Shen, C. Ultra-Stretchable Porous Fiber-Shaped Strain Sensor with Exponential Response in Full Sensing Range and Excellent Anti-Interference Ability toward Buckling, Torsion, Temperature, and Humidity. *Adv. Electron. Mater.* **2019**, *5*, 1900538.
(50) Wang, X.; Sun, H.; Yue, X.; Yu, Y.; Zheng, G.; Dai, K.; Liu, C.; Shen, C. A Highly Stretchable Carbon Nanotubes/Thermoplastic Polyurethane Fiber-Shaped Strain Sensor with Porous Structure for Human Motion Monitoring. *Compos. Sci. Technol.* **2018**, *168*, 126−132.
(51) Pan, J.; Hao, B.; Song, W.; Chen, S.; Li, D.; Luo, L.; Xia, Z.; Cheng, D.; Xu, A.; Cai, G.; Wang, X. Highly Sensitive and Durable Wearable Strain Sensors from a Core-Sheath Nanocomposite Yarn. *Compos. B Eng.* **2020**, *183*, 107683.
(52) Sun, S.; Liu, Y.; Chang, X.; Jiang, Y.; Wang, D.; Tang, C.; He, S.; Wang, M.; Guo, L.; Gao, Y. A Wearable, Waterproof, and Highly Sensitive Strain Sensor Based on Three-Dimensional Graphene/Carbon Black/Ni Sponge for Wirelessly Monitoring Human Motions. *J. Mater. Chem. C* **2020**, *8*, 2074−2085.
(53) Libanori, R.; Erb, R. M.; Reiser, A.; le Ferrand, H.; Süess, M. J.; Spolenak, R.; Studart, A. R. Stretchable Heterogeneous Composites with Extreme Mechanical Gradients. *Nat. Commun.* **2012**, *3*, 1265.
(54) Yu, M.-F.; Lourie, O.; Dyer, M. J.; Moloni, K.; Kelly, T. F.; Ruoff, R. S. Strength and Breaking Mechanism of Multiwalled Carbon Nanotubes Under Tensile Load. *Science* **2000**, *287*, 637−640.
(55) Mosadegh, B.; Polygerinos, P.; Keplinger, C.; Wennstedt, S.; Shepherd, R. F.; Gupta, U.; Shim, J.; Bertoldi, K.; Walsh, C. J.; Whitesides, G. M. Pneumatic Networks for Soft Robotics That Actuate Rapidly. *Adv. Funct. Mater.* **2014**, *24*, 2163−2170.
(56) Mai, H.; Mutlu, R.; Tawk, C.; Alici, G.; Sencadas, V. Ultra-Stretchable MWCNT−Ecoflex Piezoresistive Sensors for Human

Motion Detection Applications. *Compos. Sci. Technol.* **2019**, *173*, 118−124.
(57) Park, M.; Kim, H.; Youngblood, J. P. Strain-Dependent Electrical Resistance of Multi-Walled Carbon Nanotube/Polymer Composite Films. *Nanotechnology* **2008**, *19*, 55705.
(58) Park, S.-J.; Kim, J.; Chu, M.; Khine, M. Highly Flexible Wrinkled Carbon Nanotube Thin Film Strain Sensor to Monitor Human Movement. *Adv. Mater. Technol.* **2016**, *1*, 1600053.
(59) Xin, Y.; Zhou, J.; Xu, X.; Lubineau, G. Laser-Engraved Carbon Nanotube Paper for Instilling High Sensitivity, High Stretchability, and High Linearity in Strain Sensors. *Nanoscale* **2017**, *9*, 10897−10905.

https://dx.doi.org/10.1021/acsanm.0c02494
ACS Appl. Nano Mater. 2020, 3, 11408−11415